Electronic Supplementary Information

A Novel Fluorescent Assay for the Ultrasensitive Detection of MiRNA-21 with Use of G-quadruplex Structures as Immobilization Material of Signal Indicator

Ze-Zhou Yang, Zhi-Bin Wen, Xin Peng, Ya-Qin Chai, Wen-Bin Liang* and Ruo Yuan*

Key Laboratory of Luminescence and Real-Time Analytical Chemistry (Southwest University), Ministry of Education, College of Chemistry and Chemical Engineering, Southwest University, Chongqing 400715, P. R. China

* Corresponding authors

E-mail address: wenbinliangasu@gmail.com (Wen-Bin Liang);

yuanruo@swu.edu.cn (Ruo Yuan)

Tel.: +86-23-68252277; Fax: +86-23-68253172

Table of Contents

Experimental Section

Chemicals and Materials. Protoporphyrin IX (PPIX), Dimethyl sulfoxide (DMSO), Tween-20, Ethylenediaminetetraacetic acid (EDTA), Na_2HPO_4, NaH_2PO_4, NaCl, Tris, LiCl and $MgCl_2$ were acquired from Sigma Chemical Co. (St. Louis, MO, U.S.A.). N-(3-Dimethylaminopropyl)-N′-ethylcarbodiimide hydrochloride (EDC) and N-Hydroxy succinimide (NHS) were obtained from Shanghai Medpep Co. (Shanghai, China). T4 DNA ligase (3 U/μL), Exonuclease I and exonuclease III, Phi29 DNA polymerase (10 U/μL) were obtained from Vazyme Biotech Company, Ltd. (Nanjing, China). The solution of deoxyribonucleoside triphosphate (dNTPs) mixture was obtained from Genview Scientific Inc. (El Monte, CA, U.S.A.). Magnetic nanobeads (MNBs) (~250 nm diameter) were purchased from Tianjin Unibead Scientific Company, Ltd. (Tianjin, China). The PPIX was dissolved in DMSO, then stored at -20°C for subsequent use. Phosphate-buffer solutions (PBS) were made up of 7.6 mM Na_2HPO_4, 2.4 mM NaH_2PO_4 and 0.15 M NaCl and then the pH was tinkered up to 8.0. TE buffer solutions (pH 8.0) were made up of 10 mM Tris-HCl, 1 mM EDTA and 15 mM $MgCl_2$ standard stock solutions. TTL buffer solutions were composed of 100 mM Tris, 1 M LiCl and 0.1% Tween-20 and then the pH was tinkered up to 8.0. All the other chemicals were analytical grade and used without further purification. The ultrapure water was purified by a water purification system with resistivity of 18.2 MΩ/cm.

The oligonucleotides (Table S1) employed in this work were custom-synthesized by Shanghai Sangon Biological Engineering Technology and Services Company, Ltd. (Shanghai, China). Before using, the hairpin nucleotides (H1, H2, H3 and H4) were

heated to 95 °C for 5 min and then progressively cooled down to room temperature to form stem-loop structure.

Table S1. Oligonucleotide sequences.

Names	Sequences (5'-3')
miRNA-21	UAG CUU AUC AGA CUG AUG UUG A
ARM1	AGT GTT AAG AAG TCC TCA GTC GAT CCA ATC TAC AGC TTT TTT TTT T-NH_2
ARM2	AGT GTT AAG AAG TCC TCA GTC GAT CCA ATC TAC AGC TTT TTT TTT TTT TTT-NH_2
ARM3	AGT GTT AAG AAG TCC TCA GTC GAT CCA ATC TAC AGC TTT TTT TTT TTT TTT TTT TT-NH_2
ARM4	AGT GTT AAG AAG TCC TCA GTC GAT CCA ATC TAC AGC TTT TTT TTT TTT TTT TTT TTT TTT T-NH_2
ARM5	AGT GTT AAG AAG TCC TCA GTC GAT CCA ATC TAC AGC TTT TTT TTT TTT TTT TTT TTT TTT TTT TTT-NH_2
ARM6	AGT GTT AAG AAG TCC TCA GTC GAT CCA ATC TAC AGC TTT TTT TTT TTT TTT TTT TTT TTT TTT TTT TTT TT-NH_2
Blocker	GGA CTT CTT AAC ACT CTA GAC CAC
Padlock	PO_4^{3-}-TTC GAG GCC CTC CCA CCC CTC CCA CCC CTG GAC
Locker	GCC TCG AAG TCC AGG G
H1	TCA ACA TCA GTC TGA TAA GCT ACT AGA GTG TTA AGA AGT CCT GTT AGC TTA TCA GAC
H2	TCT GAC TAC AAC TGG ACT TCT TAA CAC TCT AGT AGC TTA TCA GAC TGA TGT TGA GTG GTC TAG AGT GTT AAG AAG TCC
H3	GAA GTC CAA ACA CAG GAC TTC TTA ACA CTA TTT TTT TTT TTT-NH_2
H4	AGT GTT AAG AAG TCC TGT GTT TGG ACT TCT TAA CAC TAC CTG AAG CTC C

miRNA-141	UAA CAC UGU CUG GUA AAG AUG G
miRNA-122	UGG AGU GUG ACA AUG GUG UUU G
miRNA-155	UUA AUG CUA AUC GUG AUA GGG GU
miRNA-182-5p	UUU GGC AAU GGU AGA ACU CAC ACU

Apparatus. The fluorescent measurements were implemented on a FL-7000 fluorescence spectrophotometer (Hitachi, Tokyo, Japan). The slit widths of both excitation and emission were set as 5 nm, and the PMT voltage was set as 950 V in all fluorescent experiments. A pH-3C digital pH-meter (Shanghai LeiCi Device Works, Shanghai, China) was employed to test the pH of all buffer solutions in the whole experiments. The gel imaging was performed by Gel Doc XR$^+$ System (Bio-Rad, California, U.S.A.).

Preparation of Circular Template. The circular template was prepared *via* an intramolecular ligation. Firstly, 1 μM Padlock and Locker was mixed at a molar ratio of 1:3. Secondly, the mixture was heated to 65 °C to keep for 10 min and progressively cooled down to room temperature for 20 min. Continuously, 10× T4 DNA ligase reaction buffer and T4 DNA ligase (3 U/μL) were added, the reaction system was incubated at 16 °C for 5 h to guarantee the intramolecular ligation of the padlock plenarily. Finally, exonuclease I and exonuclease III were added into reaction system to shear cut the extra nucleotides at 37 °C for 1 h and then inactivated at 85 °C for 15 min to obtain circular templates.

The Construction of Three-Dimensional DNA Walker. The carboxyl-MNBs were functionalized with H3 and ARM-Blocker hybrids through the literature procedures with some modifications. Briefly, 20 μL 0.5% (*w/V*) carboxyl-MNBs solutions were

washed three times with TTL buffer and resuspended in 200 μL PBS buffer. Subsequently, MNBs suspension was added into 100 μL of a mixture of EDC and NHS (4:1) and stirred 40 min to activate the carboxyl of MNBs. Next, 40 μL H3 was mixed with 80 μL ARM-Blocker hybrids and then added into the 120 μL activated MNBs suspension. The ultimate solution was incubated at room temperature for 3 h to obtain DNA-functionalized MNBs suspension. The resulting product was performed magnetic separation and washed twice with PBS buffer. After washing, the DNA-functionalized MNBs were resuspended in 120 μL PBS buffer and stored at -20 °C for the subsequent use.

Target Recycling, RCA Reaction and Fluorescent Measurements. The different concentrations of miRNA-21 (1, 2, 5, 10, 25, 50, 100, 300 and 1000 fM), H1 (1 μM) and H2 (1 μM) were mixed and reacted at 37 °C for 2 h to achieve target recycling, which could export numerous H1-H2 hybrids to hybridize with Blocker on MNBs surface. DNA-functionalized MNBs suspension and H4 was added to the target recycling reaction system to initiate the DNA walker amplification by the DNA walker self-assembly. Instantly, the RCA reaction was imitated by combination of exposed sticky ends of H4 and circular template in the solution with 2.5 U Phi29 DNA polymerase and 600 μM dNTPs. Then, the reaction solution was incubated at 30 °C for 2.0 h to produce reduplicated oligonucleotides sequences with a large number of G-quadruplexes. With the accomplishment of RCA reaction, the final products (20 μL) were incubated with 8 μL KCl (100 mM) and 5 μL PPIX (50 μM) at 37 C° for 40 min. Fluorescent data was collected from 600 nm to 670 nm on excitation of 410 nm.

The max fluorescence emission at 634 nm was employed as the indicator to estimate the capability of the miRNA-21 detection approach.

Cell Culture and Cell Lysate Preparation. Human breast cancer cells (MCF-7 cells) and human cervical cancer cells (HeLa cells) were selected to carry out the practical tests. HeLa and MCF-7 cells were cultured in DMEM medium containing 1% non-essential amino acids, 100 U/mL penicillin and 10% fetal bovine serum (FBS) at 37 °C with a humidified atmosphere (95% air and 5% CO_2). After 24 h cultivation, 10^6 cells were collected in the exponential phase and washed twice with sterile PBS. The total RNA extraction for the real sample detection was obtained using the Trizol Reagent Kit (Sangon, Inc., Shanghai, China) according to the manufacturer's protocol. Finally, the obtained cellular extracts were diluted and stored at -20 °C for further use.

Native Polyacrylamide Gel Electrophoresis (PAGE). Firstly, 10 μL of each sample was mixed with 2 μL of 6× loading buffer. And then, the mixture was transferred into notches of the freshly prepared native polyacrylamide gel (16%), respectively. Electrophoresis was implemented in 1× TBE (pH 8.0) at a 120 V constant voltage for 120 min. After staining with ethidium bromide (EB) for 15 min, the gel was transferred to Gel Doc XR^+ System for gel imaging to obtain the electrophoresis results.

Feasibility of the Proposed Strategy by UV-*vis* Spectrum and Transmission Electron Microscopy (TEM).

The UV-*vis* spectrum and transmission electron microscopy (TEM) was performed to approve the formation of MNBs@RCA products conjugates. As shown

in Figure S1A, the pure MNBs suspension did not exhibit any evident absorption peak in the wavelength scope (curve a). With the accomplishment of RCA reaction, an obvious characteristic absorption peak of DNA located at 259 nm was observed (curve b). The UV-*vis* spectra results preliminarily revealed that the successful formation of the MNBs@RCA products conjugates. As shown in Figure S1B, pure MNBs suspension exhibited relatively smooth surfaces with the size of 200 nm approximately. After reacting RCA reaction on the surface of MNBs, An apparent floccules was wrapped on the surface of MNBs (Figure S1C). The remarkable comparisons indicated that the RCA products were successfully covered on surface of MNBs.

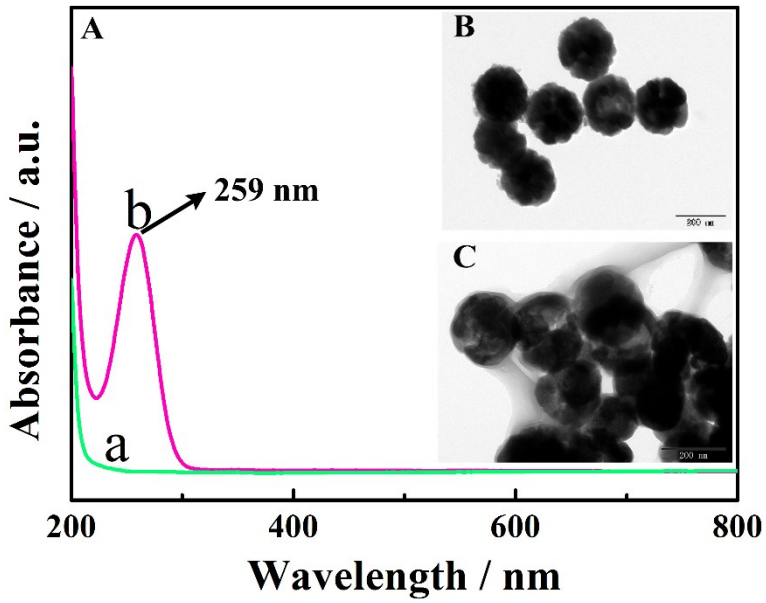

Figure S1. (A) UV-*vis* absorption spectra of MNBs (curve a) and MNBs@RCA products conjugates (curve b). (B)The TEM images of MNBs (scale bar = 200 nm). (C) The TEM images of MNBs@RCA products conjugates(scale bar = 200 nm).

Practicability of the Proposed Strategy by PAGE.

PAGE was employed to authenticate the reaction mechanism of the proposed fluorescent assay based on cascade signal amplification strategy *via* target recycling triggering three-dimensional DNA walker-assisted RCA. As shown in Figure S2, a bright single band could be clearly observed in lane 3 with lower mobility, suggesting that the target recycling was triggered to generate the hybrids between target miRNA-21 (lane 1) and H1 (lane 2). The stable formation of the H1 with H2 in lane 5, which was authenticated by the band with mobility lower than H1 in lane 2 and H2 in lane 4. Lane 6 and lane7 represented Blocker, ARM, respectively. Lane 8 represented the hybrids of ARM and Blocker. Lanes 9, 10, 11 and 12 represented Padlock, Locker, H3 and H4, respectively. Lane 13 and lane 14 illustrated the PAGE results for the proposed assay with and without target miRNA-21, respectively. As expected, on the top of lane 13, the bright band with extremely low mobility represented RCA products, and the other bands represented the ongoing detection process. However, in the absence of target miRNA-21, no obvious band could be observed on the top of lane 14, indicating that three-dimensional DNA walker was not triggered. The electrophoresis results proved the reliability and feasibility of the proposed strategy that three-dimensional DNA walker-assisted RCA was initiated in the presence of miRNA-21.

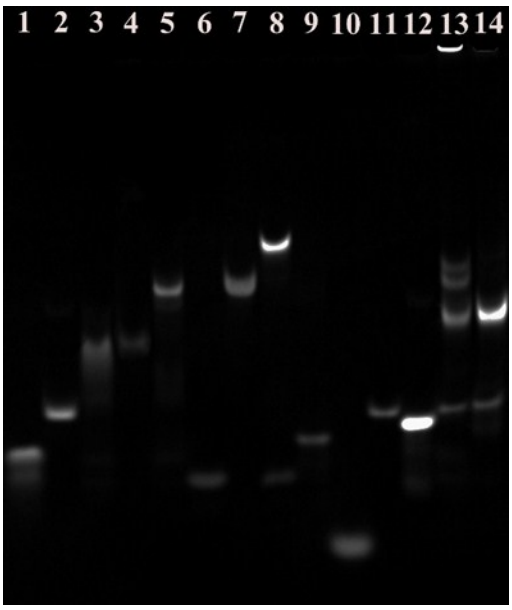

Figure S2. Native 16% PAGE analysis of the proposed fluorescent assay. Lane 1: miRNA-21; lane 2: H1; lane 3: miRNA-21 with H1; lane 4: H2; lane 5: H1 with H2; lane 6: Blocker; lane 7: ARM; lane 8: Blocker with ARM; lane 9: Padlock; lane 10: Locker; lane 11: H3; lane 12: H4; lane 13 and lane 14 were the proposed assay with and without miRNA-21, respectively.

Optimization of the Experimental Conditions.

The experimental parameters could affect the detection efficiency and performance of the proposed fluorescent assay. Herein, a range of significant influencing factors were optimized based on the fluorescent determination of miRNA-21, including the dosage of Phi29 DNA polymerase, the RCA reaction time, the concentration of K^+, the concentration of PPIX and the length of ARM.

The effect of different dosage of Phi29 DNA polymerase on the fluorescence spectrum response was investigated from 0.5 U to 3 U as shown in Figure S3A. The results indicated that the fluorescent signal intensity increased rapidly with gradually increasing dosage of Phi29 DNA polymerase and then remained approximately constant after 2.5 U. The dosage of 2.5 U was therefore employed as the optimal

dosage for subsequent experiments.

To investigate the effect of the RCA reaction time, the proposed fluorescent assay was used for the detection of miRNA-21 with incubation time from 0.5 to 3 h. As shown in Figure S3B, the fluorescent signal expeditiously increased with incubation times and then tended to be steady state after 2 h. Therefore, a topgallant incubation time of 2 h was employed for the consecutive fluorescent assays in this study.

The concentration of K^+ was a vital element for the detection efficiency and performance of the proposed strategy. Appropriate amount of K^+ can promote the massive G-rich oligonucleotides sequences to transform into a large number of G-quadruplex structures, which could combine with more luminous substances PPIX to remarkably enhance the sensitivity of detection. The fluorescent response at different concentrations of K^+ was investigated from 5 to 200 mM (Figure S3C). The fluorescent signal intensity reached a peak when the concentration of K^+ was 100 mM, indicating the optimum performance for the detection of miRNA-21.

For the label-free fluorescent strategy, the concentration of luminous substances PPIX was another extremely momentous factor. G-quadruplex structures with a higher affinity toward PPIX led to a significant enhancement of PPIX fluorescence, which was investigated based on the fluorescence spectrum response with different concentrations of PPIX between 2.5 to 100 μM (Figure S3D). The fluorescent signal increased rapidly with increasing the concentrations of PPIX and reached an equilibration state when the concentration of PPIX was 50 μM. Thus, the

concentration of PPIX of 50 μM was used as topgallant concentration for all subsequent assays.

The length of the ARM was the key factor of walking operation for the detection efficiency and performance of the proposed strategy. So the performance of the sensing system that constructed to have varying lengths of ARM (46, 51, 56, 61, 66 or 71 nt) was investigated as shown in Figure S3E. The experiment results indicated that the fluorescent signal intensity increased rapidly with gradually increasing the length of the ARM and then began to decrease after 61 nt. The length of the linker between AMR and the bead would influence the capacity of hybridization. 61 nt ARMs could provide sufficient spatial distance to reach most anchorages on the track. Therefore, the topgallant length of 61 nt was chosen for subsequent experiments.

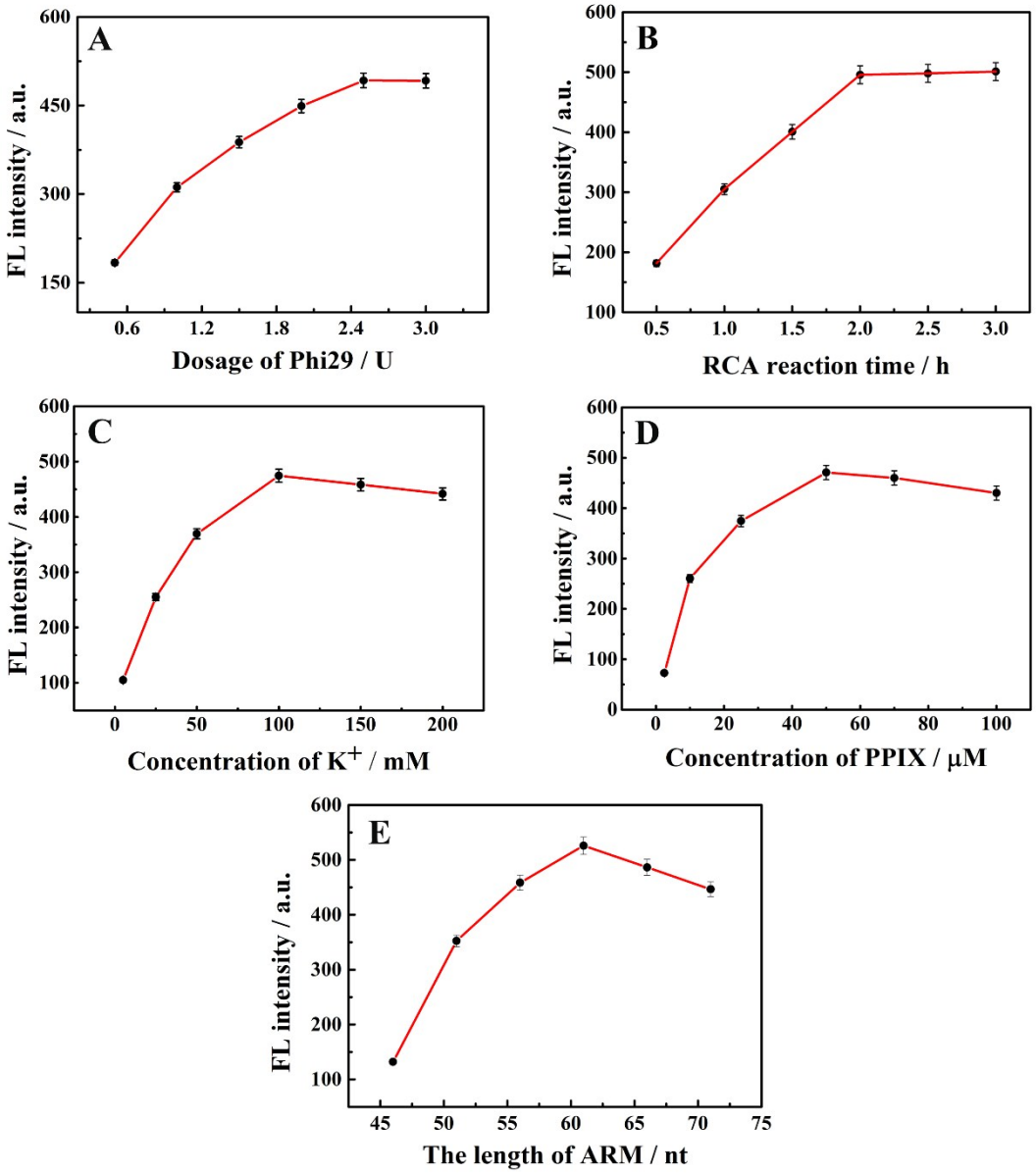

Figure S3. Relationship between the fluorescent intensity and (A) the Phi29 DNA polymerase dosage, (B) the RCA reaction time, (C) the concentration of K^+, (D) the concentration of PPIX, (E) the length of the ARM on the excitation of 410 nm and solvent of TE buffer. The detection system were incubated with KCl and PPIX at 37 °C for 40 min. Error bars represented standard deviations of three experiments.

Table S2. Comparison of the Proposed Fluorescent Assay with Other miRNA-21-Detection Strategies

Analytical methods	LOD	Linear range	Ref
Chronocoulometry	30 fM	2 fM-1 nM	1
Raman Scattering	10 fM	10 fM-100 pM	2
Electrochemistry	40 fM	0.14 nM-10 nM	3
Fluorescence	18 pM	0.05 nM-10 nM	4
Fluorescence	34 pM	0.1 nM-4 nM	5
Fluorescence	0.35 fM	1 fM-1 pM	this work

References:

1. C. S. Fang, K. S. Kim, B. Yu, S. Jon, M. S. Kim and H. Yang, *Anal. Chem*., 2017, **89**, 2024-2031.
2. J. Su, D. F. Wang, L. Nörbel, J. L. Shen, Z. H. Zhao, Y. Z. Dou, T. H. Peng, J. Y. Shi, S. Mathur, C. H. Fan and S. P. Song, *Anal. Chem*., 2017, **89**, 2531-2538.
3. S. Campuzano, R. M. Torrente-Rodríguez, E. López-Hernández, F. Conzuelo, R. Granados, J. M. Sánchez-Puelles and J. M. Pingarrón, *Angew. Chem. Int. Ed*., 2014, **53**, 6168-6171.
4. Z. B. Wen, W. B. Liang, Y. Zhuo, C. Y. Xiong, Y. N. Zheng, R. Yuan and Y. Q. Chai, *Chem. Commun*., 2018, **54**, 10897-10900.
5. H. M. Fang, N. L. Xie, M. Ou, J. Huang, W. S. Li, Q. Wang, J. B. Liu, X. H. Yang and K. M. Wang, *Anal. Chem*., 2018, **90**, 7164-7170.